ISSN: 1692-7257 - Volume 2 – Number 48 - 2026

RCTA
Revista Colombiana de Tecnologías de Avanzada
UNIPAMPLONA

Digital Object Identifier: 10.24054/rcta.v2i48.4391

Multi-species mathematical modeling and dynamic simulation of a microbial electrolysis cell for biohydrogen production

Modelado matemático multiespecie y simulación dinámica de una celda de electrólisis microbiana para la producción de biohidrógeno

PhD. Juan Carlos Quintero Díaz[1], PhD. Diego Fernando Mendoza Muñoz[1]

[1] ***Universidad de Antioquia,*** *Departamento de Ingeniería Química, Medellín, Antioquia, Colombia.*

Correspondence: *carlos.quintero@udea.edu.co*

Received: *march 27, 2025.* ***Accepted:*** *june 12, 2026.* ***Published:*** *july 02, 2026.*

How to cite: *J. C. Quintero Díaz and D. F. Mendoza Muñoz, "Multi-species mathematical modeling and dynamic simulation of a microbial electrolysis cell for biohydrogen production", RCTA, vol. 2, n.º. 48, pp. 19–29, jul. 2026. Recovered from https://ojs.unipamplona.edu.co/index.php/rcta/article/view/4391*

Abstract: A multi-population mathematical model was developed to analyze hydrogen production in Microbial Electrolysis Cells (MECs) under continuous operation. The model, implemented in Python, integrates the dynamics of fermentative, methanogenic, and exoelectrogenic bacteria with the electrochemical phenomena of the cell, and enabled assessment of the effects of applied voltage and substrate concentration on system performance. The results from the model show that exoelectrogenic bacteria form a mature biofilm that reduces the internal resistance of the cell, achieving hydrogen flow rates of 400 mL/d at 1.0 V and a Coulombic efficiency of 60%. The findings derived from the model represent a relevant contribution toward the optimization and industrial scale-up of this technology.

Keywords: hydrogen, microbial electrolysis cells, methane, Coulombic efficiency, mathematical modelling.

Resumen: Se desarrolló un modelo matemático multipoblacional para analizar la producción de hidrógeno en Celdas de Electrólisis Microbiana (CEM) en operación continua. El modelo, implementado en Python, integra la dinámica de bacterias fermentativas, metanogénicas y electrogénicas con los fenómenos electroquímicos de la celda, y permitió evaluar el efecto del voltaje aplicado y la concentración de sustrato sobre el desempeño del sistema. Los resultados del modelo muestran que las bacterias electrogénicas forman una biopelícula madura que reduce la resistencia interna de la celda, alcanzando flujos de hidrógeno de 400 mL/d a 1,0 V y una eficiencia coulómbica del 60%. Los hallazgos derivados del modelo constituyen una contribución relevante para la optimización y el escalamiento industrial de esta tecnología.

Palabras clave: hidrógeno, celdas de electrólisis microbianas, metano, eficiencia Coulómbica, modelado matemático.

1. INTRODUCTION

The intensive use of fossil fuels represents the primary cause of environmental degradation, generating diverse human health problems and adverse effects on ecosystems [1], [2]. Currently, the global energy matrix remains over 80% dependent on non-renewable sources such as oil, coal, and natural gas [3]. In this scenario, hydrogen (H_2) emerges as a strategic energy vector, with projections suggesting it could supply 10% of global energy consumption by the year 2050 [4]. However, the current challenge lies in its production method: 96% of global hydrogen production is derived from thermochemical processes utilizing fossil fuels, such as steam methane reforming [5]. Microbial Electrolysis Cell (MEC) technology emerges as an innovative alternative. These cells enable hydrogen production with significantly lower energy consumption compared to conventional water electrolysis [6].

The operating principle of a Microbial Electrolysis Cell (MEC) is based on the metabolic activity of electrogenic bacteria. These microorganisms oxidize organic matter and transfer the resulting electrons to the anode of an electrochemical circuit. Subsequently, through the application of an external voltage (typically between 0.3 and 1.0 V), the electrons migrate to the cathode, where the protons (H^+) present in the medium are reduced to produce gaseous hydrogen (H_2) [7], [8]. The viability of MECs is enhanced by using wastewater from various sources—urban, agricultural, dairy, and industrial—as low-cost substrates for hydrogen generation. It has been determined that wastewater contains between 3 and 10 times the energy required for its own treatment, primarily stored as organic matter (approx. 1.79 kWh/m^3), nutrients, and thermal energy [9], [10], [11].

In an MEC, reported hydrogen production values range between 0.01–3.9 m^3H_2/m^3.d when using acetate with an applied voltage of 1.0 V [12], [13]. Despite its potential, the use of wastewater in an MEC requires an analysis of the variables affecting its efficiency and scalability [14]. In this context, mathematical modeling serves as a tool to understand the dynamic relationship between organic matter biodegradation, microbial population growth, and the electrochemical phenomena occurring within an MEC. The mathematical description of these processes is essential for the design, optimization, and industrial scaling of this technology [15], [16].

The proposed models for microbial electrolysis cells (MECs) are based on electrochemical and biological principles that were previously applied to microbial fuel cells (MFCs). Historically, most modeling efforts have focused on MFCs [17], [18], [19]; however, models have also been developed for MECs [16], microbial electrosynthesis cells [20], and microbial desalination cells [21]. These models are generally based on ordinary differential equations describing species mass balances, incorporating Monod-type kinetics together with Faraday's law and the Nernst equation as the fundamental electrochemical frameworks.

Models have evolved to include not only temporal dynamic analyses (0D), but also one-, two-, and three-dimensional (1D, 2D, and 3D) approaches that employ partial differential equations to investigate the spatial distribution of substrates and biomass [22], [23]. Furthermore, the operation of these bioelectrochemical systems has been modeled under batch, fed-batch, and continuous operating conditions [16], [24], [25]. Both single-chamber configurations without membranes [19], [26] and two-chamber systems [27], [28] have been described in the literature. In addition, models have incorporated pure cultures to simulate the behavior of electroactive microorganisms such as *Shewanella* spp. and *Geobacter sulfurreducens* [18], [22], [27], as well as multispecies systems representing microbial consortia, such as those found in anaerobic sludge [16], [23]. Electron transfer mechanisms have also been integrated into these models, including direct electron transfer pathways [22], as well as intracellular mediator-based [16] and extracellular mediator-based electron transfer mechanisms [18]. The model proposed by Pinto et al. [16] was the first dynamic multipopulation model capable of simulating hydrogen (H_2) production from complex organic matter in a single-chamber microbial electrolysis cell (MEC) operated under continuous conditions. The model employs a system of ordinary differential equations to describe the growth and metabolic activity of four interacting microbial populations forming a biofilm on the electrode surfaces. Table 1 summarizes the most important factors that have been considered in the modeling of microbial electrochemical systems.

The highly nonlinear behavior resulting from the complex interactions occurring within bioelectrochemical systems presents considerable challenges for parameter estimation and control design. To address these limitations, hybrid modeling approaches combining mechanistic descriptions with machine learning techniques,

particularly recurrent neural networks, have emerged as attractive alternatives for enhancing predictive capabilities and real-time process control [29], [30], [31]. Nevertheless, the inherent black-box nature of such methods restricts their physical interpretability. Therefore, the development of more comprehensive models that integrate biofilm processes, mass and charge transport dynamics, and reactor performance remains a key requirement for enabling the rational design, optimization, and scale-up of microbial electrolysis cells.

Table 1: *Factors considered in mathematical models of microbial electrolysis cells (MECs).*

Criterion	Options			This work
Dimension	0D	1D / 2D / 3D		0D
Chamber configuration	Anode	Cathode	Anode/Cathode	Anode/Cathode
Electron transfer (EET)	Direct	Endogenous mediator	Exogenous mediator	Endogenous mediator
Microbial culture	Pure	Two-species	Microbial consortium	Microbial consortium
Mode of operation	Batch	Fed-batch	Continuous	Continuous

In this study, a mathematical model is developed to integrate the three aforementioned phenomena in a continuously operated dual-chamber microbial electrolysis cell (MEC). The proposed framework is intended to characterize the dynamic behavior of the system and to assess the influence of operating variables, including the applied voltage and organic substrate loading, on hydrogen production and the Coulombic efficiency of the reactor.

2. METHODOLOGY

2.1. MEC Description

The mathematical model presented in this study is based on the framework proposed by Pinto et al. [16] and was adapted to represent a dual-chamber microbial electrolysis cell (MEC) (Figure 1). Unlike the model proposed by Pinto et al., the cathode does not contain a microbial biofilm; therefore, neither H_2 consumption nor CH_4 production occurs. Additionally, the model assumes that the biomass is present both as suspended flocs and as a biofilm attached to the anode. Consequently, the fraction of biomass leaving the system through the effluent is represented by the parameter α (Equations 3–5).

Wastewater enters the anodic chamber containing organic matter, represented by glucose (*S*) and acetate (*A*), and leaves as effluent with a significant reduction in organic content. The anaerobic sludge is either attached to the electrode forming a biofilm or is in suspension within the medium. This sludge consists of three types of bacterial species: fermentative (x_f), methanogenic (x_m), and electrogenic (x_e), listed in descending order of their proportion within the biomass. These species perform the following conversion reactions:

Glucose conversion into acetate by fermentative bacteria (x_f):

$$C_6H_{12}O_6\ (S) \rightarrow 3C_2H_4O_2\ (A)$$

Acetate consumption by methanogenic bacteria (x_m):

$$C_2H_4O_2\ (A) \rightarrow CH_4 + CO_2$$

Acetate consumption by electrogenic bacteria (x_e):

$$C_2H_4O_2\ (A) + 2H_2O + 4Mox \rightarrow 4Mred + 2CO_2$$

In this last reaction, electrogenic bacteria are considered to produce an endogenous redox mediator (M) that facilitates electron transfer from the cell interior to the anode [32], [33], [34].

The electrons delivered by the electrogenic bacteria to the anode are driven by an external power source toward the cathode. Meanwhile, the protons released during the oxidation of organic matter flow toward the cathode through a semipermeable membrane that separates the two chambers. The hydrogen evolution reaction at the cathode is as follows:

$$2H^+ + 2e^- \rightarrow H_2(g)$$

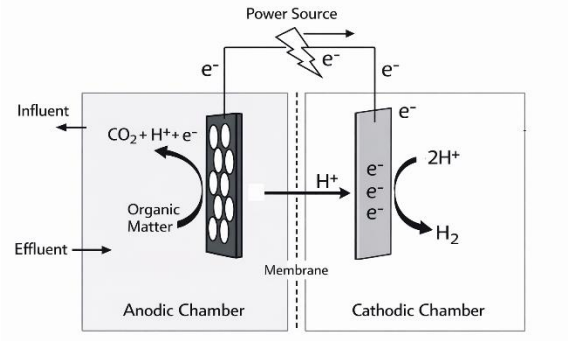

Fig. 1*. Schematic diagram of a dual-chamber microbial electrolysis cell (MEC) for hydrogen production*

The theoretical thermodynamic cell potential (E_{CEF}) of a microbial electrolysis cell (MEC) for hydrogen production at pH 7.0 is -0.14 V; therefore, the reaction is non-spontaneous and requires an external potential greater than 0.14 V for hydrogen production to occur. However, cell overpotentials

force the application of a higher voltage, typically ranging from 0.2 to 1.0 V [6].

2.2. Model Development

The mass balances for an MEC in continuous flow (Figure 1) are described in Equations 1–7. For the cell balance, it is assumed that the microorganisms do not leave the reactor, as they are either attached to the electrode or undergo settling within the medium.

Susbtrate mass balance (S)

$$\frac{dS}{dt} = -q_f x_f + D(S_0 - S) \quad \text{Eq. 1}$$

Acetate mass balance (A):

$$\frac{dA}{dt} = -q_e x_e - q_m x_m + Y_{COD} q_f x_f + D(A_0 - A) \quad \text{Eq. 2}$$

Fermentative bacteria mass balance (x_f)

$$\frac{dx_f}{dt} = \mu_f x_f - K_{df} x_f - \alpha x_f \quad \text{Eq. 3}$$

Acetoclastic methanogenic bacteria mass balance (x_m)

$$\frac{dx_m}{dt} = \mu_m x_m - K_{dm} x_m - \alpha x_m \quad \text{Eq. 4}$$

Electrogenic bacteria mass balance (x_e)

$$\frac{dx_e}{dt} = \mu_e x_e - K_{de} x_e - \alpha x_e \quad \text{Eq. 5}$$

Endogenous redox mediator mass balance (M)

$$M_{Total} = M_{red} + M_{ox} \quad \text{Eq. 6}$$

$$\frac{dM_{ox}}{dt} = -Y_M q_e + \frac{\gamma}{V x_e} \frac{I_{MEC}}{nF} \quad \text{Eq. 7}$$

Growth kinetics (μ_i) and substrate consumption rates (q_i) based on the Monod model correspond to Equations 8–13

$$\mu_f = \mu_{max,f} \frac{S}{K_{s,f} + S} \quad \text{Eq. 8}$$

$$\mu_e = \mu_{max,e} \frac{A}{K_{A,e} + A} \quad \text{Eq. 9}$$

$$\mu_m = \mu_{max,m} \frac{A}{K_{A,m} + A} \quad \text{Eq. 10}$$

$$q_f = q_{max,f} \frac{S}{K_{s,f} + S} \quad \text{Eq. 11}$$

$$q_e = q_{max,e} \frac{A}{K_{A,e} + A} \quad \text{Eq. 12}$$

$$q_m = q_{max,m} \frac{A}{K_{A,m} + A} \quad \text{Eq. 13}$$

The electrochemical cell balance is described in Equations 14–19, where the applied voltage $E_{app.}$ must be sufficient to cover the thermodynamic potential E_{CEF}. The ohmic overpotential (η_{ohm}) based on Ohm's law, represents the energy lost as heat due to the resistance of ions moving through the liquid (electrolyte) and the membrane, and electrons through the wires and electrodes. The anodic overpotential (η_a) based on the Nernst equation applied to the biological mediator, represents the potential loss occurring from limitations in the mediator reduction rate. Meanwhile, the cathodic overpotential (η_c) is a form of the Butler–Volmer equation representing the energy required to maintain the chemical reaction at the cathode surface. R_{int} is represented by an empirical model proposed by Marcus et al. (2007) [35], which suggests that internal resistance decreases as the electrogenic biomass on the anode increases.

$$-E_{aplic.} = E_{CEF} - \eta_{ohm} - \eta_a - \eta_c \quad \text{Ec. 14}$$

$$\eta_{ohm} = I_{MEC} * R_{int} \quad \text{Ec. 15}$$

$$\eta_a = \frac{RT}{nF} ln\left(\frac{M_{total}}{M_{red}}\right) \quad \text{Ec. 16}$$

$$\eta_c = \frac{RT}{\beta_m F} \sinh^{-1}\left(\frac{I_{MEC}}{A_c\, i_0}\right) \quad \text{Ec. 17}$$

$$I_{MEC} = \frac{E_{CEF} + E_{app.} - \eta_a - \eta_c}{R_{int}} \quad \text{Ec. 18}$$

$$R_{int} = R_{min} + (R_{max} - R_{min})\, e^{-K_R x_e} \qquad \text{Ec. 19}$$

The methane production rate (Q_{CH4}) in the anodic chamber and the hydrogen production rate (Q_{H2}) in the cathodic chamber are represented by Equations 20 and 21.

$$Q_{CH4} = Y_{CH4}\, q_m\, x_m\, V \qquad \text{Ec. 20}$$

$$Q_{H2} = Y_{H2} \left(\frac{I_{MEC}}{nF} \frac{RT}{P}\right) \qquad \text{Ec. 21}$$

The kinetic and electrochemical parameters used in the model were adapted from the validated parameter set reported by Pinto et al. [16] and are summarized in Table 2.

2.3. Numerical solution of the model

The system of ordinary differential equations (ODEs) was solved through numerical computing in a Python environment, using the variable-step integration algorithm odeint from the SciPy library.

Table 2: *Model Parameters*

Parameter	Descripción	Value
$\mu_{max,f}$ (1/d)	Max.specific growth rate	0.15
$\mu_{max,e}$ (1/d)	Max.specific growth rate	0.25
$\mu_{max,m}$ (1/d)	Max.specific growth rate	0.1
$K_{s,f}$ (mg/L)	Half-saturation constant	100
$K_{s,e}$ (mg/L)	Half-saturation constant	20
$K_{s,m}$ (mg/L)	Half-saturation constant	80
$q_{max,f}$ (1/d)	Max.substrate uptake rate	16.0
$q_{max,e}$ (1/d)	Max.substrate uptake rate	14.0
$q_{max,m}$ (1/d)	Max.substrate uptake rate	14.0
$K_{d,f}$ (1/d)	Decay rate coefficient	0.01
$K_{d,e}$ (1/d)	Decay rate coefficient	0.01
$K_{d,m}$ (1/d)	Decay rate coefficient	0.01
α (1/d)	Biomass washout rate	0.1
Y_{COD} (mg/mg)	Acetate-to-glucose yield	0.75
Y_M (mg/mg)	Oxidized mediator yield	36.6
Y_{H2} (-)	Cathodic efficiency	0.8
Y_{CH4} (L/mg)	Methane yield coefficient	0.28
γ (-)	Electron transfer efficiency	1.0
E_{CEF} (V)	Electromotive force	-0.3
Eapp (V)	Applied cell voltage	0.8
R_{min} (Ohm)	Min. internal resistance	20
R_{max} (Ohm)	Max. internal resistance	2000
K_r (L/mg)	Biomass resistance decay	0.024
F (C/mol e)	Faraday constant	96485
n (mol e/mol)	Electrons transferred	2
R (J/mol K)	Ideal gas constant	8.314
T (K)	Temperature	303.15
P (Pa)	Pressure	101325
M_{total} (M)	Total mediator conc.	0.05
V_{liq} (L)	Liquid volume	1.0
D (1/d)	Dilution rate	0.5
S_0 (mg/L)	Influent substrate conc.	3000
A_0 (mg/L)	Influent acetate conc.	10
β_m(-)	Cathodic charge transfer	0.5
AC (m^2)	Cathode surface area	0.22
i_0 (A/m^2)	Exchange current density	1.0

Source: The parameter values were adopted based on the orders of magnitude reported by Pinto et al. [16].

To assess the influence of model parameters on hydrogen production, a local sensitivity analysis was conducted by perturbing each parameter individually by 1% relative to its nominal value. The resulting dynamic responses were normalized and quantified using the Root Mean Square (RMS) metric over the simulation period. Subsequently, the parameters were ranked according to their sensitivity indices and represented in a Pareto chart to facilitate the identification of the most influential variables affecting system performance [36], [37]. The initial conditions for the dynamic variables were as follows: So = 1000 mg/L; Ao = 10 mg/L; x_{fo}=50 mg/L; x_{mo}= 20 mg/L; x_{eo}= 5 mg/L; M_{ox}= 0.02 mg/L. The model solution was carried out at a dilution rate (D) of 0.5 1/d, with a volume (V) of 1 L in each cell chamber. The model was used to evaluate the effect of applied voltage and substrate concentration on H_2 production, the H_2 yield from substrate ($Y_{H_2/S}$), and the Coulombic efficiency (CE). These variables are defined in Equations 22 and 23. To determine which parameters exert the greatest influence on the output variables (Q_{H2} y EC), a global sensitivity analysis was performed based on the root mean square (RMS) of the normalized sensitivities [36], [37].

$$Y_{H_2/S} = \frac{Q_{H2}}{D(So - S)} \qquad \text{Ec. 22}$$

$$EC = \frac{I_{MEC}}{n\, F q_e\, x_e\, V} \qquad \text{Ec. 23}$$

3. RESULTS AND DISCUSSION

Figures 2–5 present the dynamic behavior of a microbial electrolysis cell (MEC), where the anodic chamber is continuously fed with wastewater containing an organic load represented by glucose and acetate. The microbial population dynamics in the anodic chamber show a clear transition from a heterogeneous inoculum toward a specialized community (Figure 2). At the beginning of the operation, the highest proportion of species corresponds to fermentative bacteria, which dominate the hydrolysis and acidogenesis stages,

transforming the complex substrate (glucose) into metabolic intermediates such as acetate (Figure 3). This initial hierarchy, where fermenters predominate over methanogens, and these, in turn, over electrogens, is characteristic of the conventional anaerobic sludge used as inoculum [38].

As the process progresses, a sigmoidal increase in the electrogenic biomass is observed (Figure 2). This growth is attributed to the thermodynamic advantage provided by the applied potential $E_{app.}$, which induces the anode to act as an electron acceptor. This allows electrogenic bacteria to achieve a growth rate superior to that of their competitors under the established operating conditions. On the other hand, the glucose turnover rate maintains an active fermentative population that consumes glucose, keeping its concentration low by transforming it into acetate. Due to glucose consumption, acetate initially tends to accumulate in the medium (Figure 3) because of the low consumption by methanogenic and electrogenic bacteria, which are present in low proportions at this stage. Under these conditions, however, methanogens consume the acetate, generating methane in significant proportions (Figure 4). Nevertheless, as electrogenic growth increases, the competition for acetate intensifies, leading to a reduction in methane production and a corresponding increase in hydrogen production (Figure 4) due to the electron transfer from the anode.

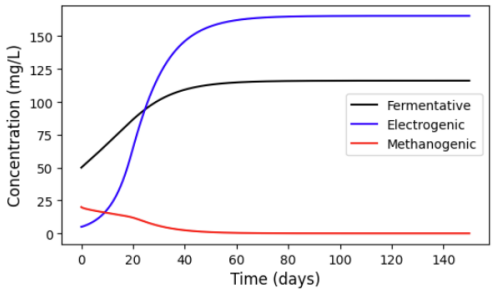

***Fig. 2**. Bacterial species behavior in the MEC anodic chambe*

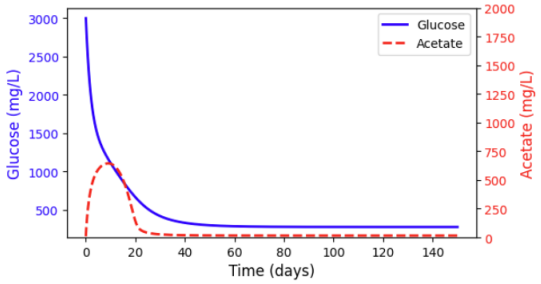

***Fig. 3**. Glucose and acetate profiles in the MEC anodic chamber*

Figure 5 illustrates the behavior of the current flow through the MEC and the internal resistance of the system. As the electrogenic bacterial population grows and forms a mature biofilm (around days 20 to 40), a drastic drop in resistance is observed, stabilizing at a minimum value near 100 Ω. This reduction in resistance enables a parallel increase in current. This phenomenon occurs because the biofilm acts as a biological catalyst that facilitates extracellular electron transfer (EET), thereby reducing the resistance to electron transfer at the anode. The adaptation of anaerobic sludge into an electrogenic population has been reported in various studies [39], [40].

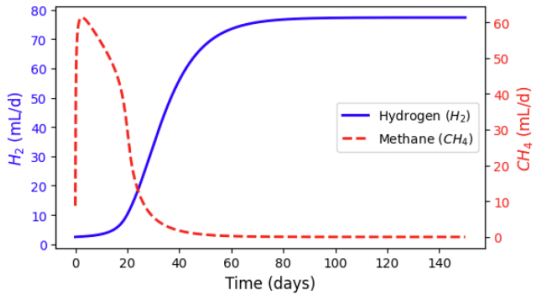

***Fig. 4**. Dynamics of methane evolution (anodic chamber) and hydrogen evolution (cathodic chamber) in an MEC*

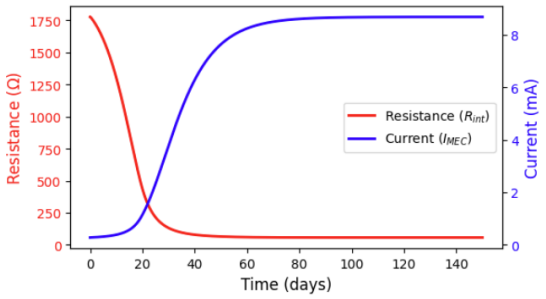

***Fig. 5**. Internal resistance behavior and current generation in an MEC during hydrogen production.*

The response surface in Figure 6 shows a clear interdependence between the applied voltage and the initial substrate concentration on hydrogen production. It is observed that voltage is the most influential factor; as it increases from 0.2 V to 1.0 V, gas production rises drastically, reaching values near 400 mL/d. This occurs because the voltage acts as the necessary thermodynamic driving force for electrons to overcome the system's overpotentials and flow from the anode to the cathode. Furthermore, increasing the substrate also favors hydrogen production, although its effect tends to stabilize as the concentration increases. This behavior is due to Monod-type saturation kinetics, where the bacteria reach their maximum metabolic processing capacity, and the substrate ceases to be

the limiting factor. In the low-voltage region, H_2 production remains minimal regardless of the amount of substrate added, demonstrating that without sufficient electrical energy, the biomass cannot effectively channel electrons toward the anode. The maximum hydrogen production is achieved at 1.0 V and between 6,000 and 8,000 mg/L, as substrate saturation and minimum internal resistance allow for the maximum current flow in the system.

The model predicted a maximum hydrogen production rate of 0.4 $m^3/m^3 \cdot d$, which is consistent with the range reported in the literature for dual-chamber microbial electrolysis cells (0.25–0.89 $m^3/m^3 \cdot d$,) [41], [42], [43]. This consistency provides additional validation for the parameter set employed in the model.

The response surface for Coulombic Efficiency (CE) (Figure 7) reveals a more complex interaction between the applied voltage and the initial substrate concentration, differing significantly from the behavior observed for hydrogen production.

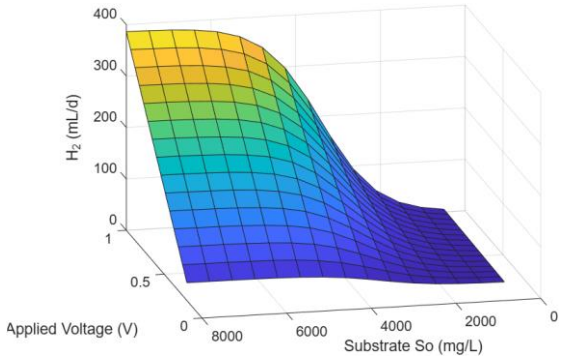

***Fig. 6**. Effect of voltage and substrate on hydrogen production in an MEC.*

It is observed that the Coulombic Efficiency (CE) reaches a maximum value of approximately 60% in a specific region of voltages near 1.0 V, combined with substrate concentrations around 4,500 mg/L. This behavior indicates that, unlike gas production, conversion efficiency requires a balance where the organic load is high enough to sustain electrogenic activity, but not so excessive as to divert electrons toward competing metabolic pathways, such as biomass accumulation.

It is noted that below and above a substrate concentration of 4,500 mg/L, the efficiency tends to decrease. This suggests that at very low concentrations, cellular maintenance consumes proportionately more energy, while at very high concentrations, the anode's electron transfer capacity reaches saturation. High voltages near 1.0 V combined with low or moderate organic loads have been observed as a strategy against methanogenic activity, favoring the growth kinetics of electrogens, where CEs between 21% and 93% have been achieved [44], [45].

The response surface analysis of the hydrogen yield based on substrate consumption ($Y_{H_2/S}$) as a function of applied voltage and substrate concentration showed a trend similar to that observed for CE. The maximum predicted yield was 150 mL/g under the same optimal operating conditions. This value is within the range reported for dual-chamber microbial electrolysis cells (135–340 mL/g) [46] and is comparable to the hydrogen yields obtained through dark fermentation processes [47], further supporting the validity of the model predictions.

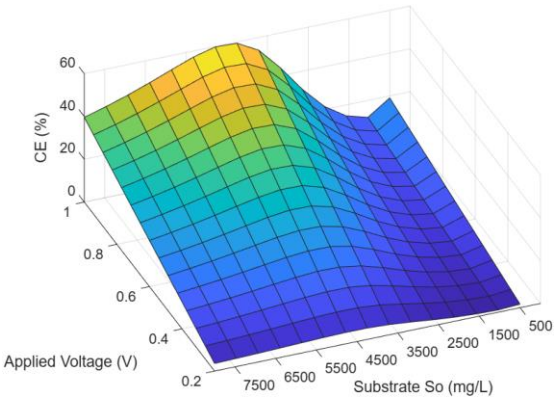

***Fig. 7**. Effect of voltage and substrate on the Coulombic Efficiency (CE) of an MEC.*

The Pareto chart in Figure 8 indicates that the electrogenic bacteria growth rate (μ_e), the initial substrate concentration (S_0), and the exponential decay constant of internal resistance due to the presence of electrogenic populations (k_r) are the three parameters with the greatest impact on hydrogen production. The microbiology and metabolism of electrogenic bacteria govern the overall cell behavior, as demonstrated by the high sensitivity of the parameters μ_e (growth rate) and q_e (consumption rate), which drive the biofilm activity at the anode. On the other hand, the initial substrate concentration S_0, along with the dilution rate D, constitute additional critical factors representing the electron flow available to the system. A limitation in this supply directly restricts hydrogen production kinetics by reducing the availability of electron donors.

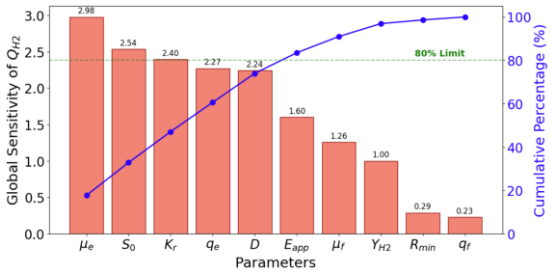

Fig. 8*. Pareto chart of model parameters with the greatest effect on hydrogen production*

The Pareto chart of the global sensitivity analysis for Coulombic Efficiency (CE) (Figure 9) reveals once again that the microbiology and biochemistry of electrogenic bacteria control the cell behavior. Specifically, the parameters μ_e and q_e, dictate the fraction of substrate that is actually converted into current, while the parameter k_r serves as a measure of the internal resistance reduction that facilitates electron transfer to the electrode. The applied voltage E_{app} represents the supplementary energy required to overcome the thermodynamic barrier for hydrogen production. This parameter is the primary modulator of reaction kinetics, as higher voltages accelerate the metabolism of the electrogenic biofilm and, consequently, the electrical current intensity. At low voltages, the driving force is weak and internal resistance dominates; this causes the electrons generated by the bacteria to be diverted toward competing pathways, such as methanogenesis or biomass synthesis, thereby reducing the CE.

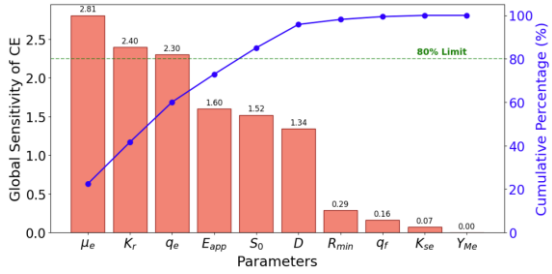

Fig. 9*. Pareto chart of model parameters with the greatest effect on Coulombic Efficiency*

4. CONCLUSIONS

Mathematical modeling is an essential tool for systems analysis, enabling the prediction of dynamic behavior and the determination of critical parameters fundamental for the design, optimization, and industrial scaling of various technologies. During the analysis of hydrogen production in a Microbial Electrolysis Cell, the primary findings included the transition of the inoculum toward a mature electrogenic biofilm. This specialized community drastically reduces internal resistance, thereby facilitating electron transfer. The applied voltage emerged as one of the most influential factors, achieving production rates of up to 400 mL/d of hydrogen at 1.0 V (0.4 $m^3/m^3 \cdot d$), with Coulombic efficiencies reaching approximately 60%. Sensitivity analyses demonstrated that parameters associated with the biochemistry of electrogenic cells, such as the growth rate and acetate consumption rate, control the overall performance of the cell. Consequently, future scaling and optimization efforts must prioritize the evaluation of these parameters to maximize energy conversion and the economic viability of the process.

Contribution of authors: Conceptualization: JCQD. y DFM.; methodology: JCQD; software: JCQD; validation: JCQD; formal analysis: JCQD. y DFM.; investigation: JCQD.; resources: JCQD.; data curation: JCQD.; writing—original draft: JCQD.; writing—review and editing: JCQD. y DFM.; visualization: JCQD. y DFM.; project administration: JCQD.; All authors have read and approved the final version of the manuscript.

Code availability: The Python code for the numerical solution of the model will be provided by the authors to interested readers upon request.

REFERENCES

[1] C. Carraro, S. Searle, and C. Baldino, 'Waste and residue availability for advanced biofuel production in the European Union and the United Kingdom', International Council on Clean Transportation, Working paper 2021-39, 2021.

[2] K. Vohra, A. Vodonos, J. Schwartz, E. A. Marais, M. P. Sulprizio, and L. J. Mickley, 'Global mortality from outdoor fine particle pollution generated by fossil fuel combustion: Results from GEOS-Chem', *Environmental Research*, vol. 195, p. 110754, Apr. 2021, doi: 10.1016/j.envres.2021.110754.

[3] T. da Silva Veras, T. S. Mozer, D. da Costa Rubim Messeder dos Santos, and A. da Silva César, 'Hydrogen: Trends, production and characterization of the main process worldwide', *International Journal of Hydrogen Energy*, vol. 42, no. 4, pp. 2018–2033, Jan. 2017, doi: 10.1016/j.ijhydene.2016.08.219.

[4] S. G. Nnabuife *et al.*, 'The prospects of hydrogen in achieving net zero emissions by 2050: A critical review', *Sustainable Chemistry for Climate Action*, vol. 2, p.

100024, Jan. 2023, doi: 10.1016/j.scca.2023.100024.

[5] M. T. Ahad, M. M. H. Bhuiyan, A. N. Sakib, A. B. Corral, and Z. Siddique, 'An Overview of Challenges for the Future of Hydrogen', *Materials*, vol. 16, no. 20, Oct. 2023, doi: 10.3390/ma16206680.

[6] B. E. Logan *et al.*, 'Microbial Electrolysis Cells for High Yield Hydrogen Gas Production from Organic Matter', ACS Publications. Accessed: Oct. 27, 2022. [Online]. Available: https://pubs.acs.org/doi/pdf/10.1021/es801553z

[7] H. Liu, S. Grot, and B. E. Logan, 'Electrochemically assisted microbial production of hydrogen from acetate', *Environ Sci Technol*, vol. 39, no. 11, pp. 4317–4320, Jun. 2005, doi: 10.1021/es050244p.

[8] P. Dange *et al.*, 'Recent Developments in Microbial Electrolysis Cell-Based Biohydrogen Production Utilizing Wastewater as a Feedstock', *Sustainability*, vol. 13, no. 16, Art. no. 16, Jan. 2021, doi: 10.3390/su13168796.

[9] Z. Dai, E. S. Heidrich, J. Dolfing, and A. P. Jarvis, 'Determination of the Relationship between the Energy Content of Municipal Wastewater and Its Chemical Oxygen Demand', *Environ. Sci. Technol. Lett.*, vol. 6, no. 7, pp. 396–400, Jul. 2019, doi: 10.1021/acs.estlett.9b00253.

[10] E. S. Heidrich, T. P. Curtis, and J. Dolfing, 'Determination of the Internal Chemical Energy of Wastewater', *Environ. Sci. Technol.*, vol. 45, no. 2, pp. 827–832, Jan. 2011, doi: 10.1021/es103058w.

[11] B. E. Logan and K. Rabaey, 'Conversion of wastes into bioelectricity and chemicals by using microbial electrochemical technologies', *Science*, vol. 337, no. 6095, pp. 686–690, Aug. 2012, doi: 10.1126/science.1217412.

[12] E. Yang *et al.*, 'A review on self-sustainable microbial electrolysis cells for electro-biohydrogen production via coupling with carbon-neutral renewable energy technologies', *Bioresource Technology*, vol. 320, p. 124363, Jan. 2021, doi: 10.1016/j.biortech.2020.124363.

[13] G. Kumar *et al.*, 'Microbial electrochemical systems for sustainable biohydrogen production: Surveying the experiences from a start-up viewpoint', *Renewable and Sustainable Energy Reviews*, vol. 70, pp. 589–597, Apr. 2017, doi: 10.1016/j.rser.2016.11.107.

[14] M. Muddasar *et al.*, 'Performance efficiency comparison of microbial electrolysis cells for sustainable production of biohydrogen—A comprehensive review', *International Journal of Energy Research*, vol. 46, no. 5, pp. 5625–5645, 2022, doi: 10.1002/er.7606.

[15] S. Gadkari, S. Gu, and J. Sadhukhan, 'Towards automated design of bioelectrochemical systems: A comprehensive review of mathematical models', *Chemical Engineering Journal*, vol. 343, no. February, pp. 303–316, 2018, doi: 10.1016/j.cej.2018.03.005.

[16] R. P. Pinto, B. Srinivasan, A. Escapa, and B. Tartakovsky, 'Multi-Population Model of a Microbial Electrolysis Cell', *Environ. Sci. Technol.*, vol. 45, no. 11, pp. 5039–5046, Jun. 2011, doi: 10.1021/es104268g.

[17] S. Gadkari, M. Shemfe, and J. Sadhukhan, 'Microbial fuel cells: A fast converging dynamic model for assessing system performance based on bioanode kinetics', *International Journal of Hydrogen Energy*, vol. 44, no. 29, pp. 15377–15386, Jun. 2019, doi: 10.1016/j.ijhydene.2019.04.065.

[18] X.-C. Zhang and A. Halme, 'Modelling of a microbial fuel cell process', *Biotechnol Lett*, vol. 17, no. 8, pp. 809–814, Aug. 1995, doi: 10.1007/BF00129009.

[19] R. P. Pinto, B. Srinivasan, M.-F. Manuel, and B. Tartakovsky, 'A two-population bio-electrochemical model of a microbial fuel cell', *Bioresource Technology*, vol. 101, no. 14, pp. 5256–5265, Jul. 2010, doi: 10.1016/j.biortech.2010.01.122.

[20] M. Kazemi, D. Biria, and H. Rismani-Yazdi, 'Modelling bio-electrosynthesis in a reverse microbial fuel cell to produce acetate from CO2 and H2O', *Phys. Chem. Chem. Phys.*, vol. 17, no. 19, pp. 12561–12574, 2015, doi: 10.1039/c5cp00904a.

[21] Q. Ping, C. Zhang, X. Chen, B. Zhang, Z. Huang, and Z. He, 'Mathematical Model of Dynamic Behavior of Microbial Desalination Cells for Simultaneous Wastewater Treatment and Water Desalination', *Environ. Sci. Technol.*, vol. 48, no. 21, pp. 13010–13019, Nov. 2014, doi: 10.1021/es504089x.

[22] S. Yao, Y.-L. He, B.-Y. Song, and X.-Y. Li, 'A two-dimensional, two-phase mass transport model for microbial fuel cells', *Electrochimica Acta*, vol. 212, pp. 201–211, Sep. 2016, doi: 10.1016/j.electacta.2016.06.167.

[23] C. Picioreanu, M. C. M. van Loosdrecht, T. P. Curtis, and K. Scott, 'Model based evaluation of the effect of pH and electrode geometry on microbial fuel cell performance',

Bioelectrochemistry, vol. 78, no. 1, pp. 8–24, Apr. 2010, doi: 10.1016/j.bioelechem.2009.04.009.

[24] Y. Azwar, A. K. Abdul-Wahab, and M. A. Hussain, 'Optimal Production of Biohydrogen Gas via Microbial Electrolysis Cells (MEC) in a Controlled Batch Reactor System'.

[25] A. M. Yahya, M. A. Hussain, and A. K. Abdul Wahab, 'Modeling, optimization, and control of microbial electrolysis cells in a fed-batch reactor for production of renewable biohydrogen gas', *International Journal of Energy Research*, vol. 39, no. 4, pp. 557–572, 2015, doi: 10.1002/er.3273.

[26] B. Sirinutsomboon, 'Modeling of a membraneless single-chamber microbial fuel cell with molasses as an energy source', *Int. J. Energy Environ. Eng.*, vol. 5, no. 2–3, pp. 1–9, 2014, doi: 10.1007/s40095-014-0093-5.

[27] Y. Zeng, Y. F. Choo, B.-H. Kim, and P. Wu, 'Modelling and simulation of two-chamber microbial fuel cell', *Journal of Power Sources*, vol. 195, no. 1, pp. 79–89, Jan. 2010, doi: 10.1016/j.jpowsour.2009.06.101.

[28] V. B. Oliveira, M. Simões, L. F. Melo, and A. M. F. R. Pinto, 'A 1D mathematical model for a microbial fuel cell', *Energy*, vol. 61, pp. 463–471, Nov. 2013, doi: 10.1016/j.energy.2013.08.055.

[29] M. N. Ikhmal Salehmin *et al.*, 'Modeling biohydrogen production from microbial electrolysis cells in the machine learning era: a review', *Sustainable Energy Technologies and Assessments*, vol. 85, p. 104819, Jan. 2026, doi: 10.1016/j.seta.2026.104819.

[30] M. A. Mohd Asrul, M. F. Atan, H. Abdul Halim Yun, and J. C. H. Lai, 'Mathematical model of biohydrogen production in microbial electrolysis cell: A review', *International Journal of Hydrogen Energy*, vol. 46, no. 75, pp. 37174–37191, Oct. 2021, doi: 10.1016/j.ijhydene.2021.09.021.

[31] A. Garg, V. Vijayaraghavan, S. S. Mahapatra, K. Tai, and C. H. Wong, 'Performance evaluation of microbial fuel cell by artificial intelligence methods', *Expert Systems with Applications*, vol. 41, no. 4, Part 1, pp. 1389–1399, Mar. 2014, doi: 10.1016/j.eswa.2013.08.038.

[32] E. M. Conners, K. Rengasamy, and A. Bose, 'Electroactive biofilms: how microbial electron transfer enables bioelectrochemical applications', *J. Ind. Microbiol. Biotechnol.*, vol. 49, no. 4, p. kuac012, Jul. 2022, doi: 10.1093/jimb/kuac012.

[33] C. Montoya-Vallejo, J. O. Gil Posada, and J. C. Quintero-Díaz, 'Enhancement of Electricity Production in Microbial Fuel Cells Using a Biosurfactant-Producing Co-Culture', *Molecules*, vol. 28, no. 23, Art. no. 23, Jan. 2023, doi: 10.3390/molecules28237833.

[34] E. Marsili, D. B. Baron, I. D. Shikhare, D. Coursolle, J. A. Gralnick, and D. R. Bond, 'Shewanella secretes flavins that mediate extracellular electron transfer', *Proceedings of the National Academy of Sciences*, vol. 105, no. 10, pp. 3968–3973, Mar. 2008, doi: 10.1073/pnas.0710525105.

[35] A. Kato Marcus, C. I. Torres, and B. E. Rittmann, 'Conduction-based modeling of the biofilm anode of a microbial fuel cell', *Biotechnology and Bioengineering*, vol. 98, no. 6, pp. 1171–1182, 2007, doi: 10.1002/bit.21533.

[36] A. Saltelli, M. Ratto, S. Tarantola, and F. Campolongo, 'Sensitivity Analysis for Chemical Models', *Chem. Rev.*, vol. 105, no. 7, pp. 2811–2828, Jul. 2005, doi: 10.1021/cr040659d.

[37] A. Varma, M. Morbidelli, and H. Wu, *Parametric sensitivity in chemical systems*, vol. 1. Cambridge University Press Cambridge, 1999. Accessed: Mar. 22, 2026. [Online]. Available: https://www.academia.edu/download/118001995/248350749.pdf

[38] W. Cai *et al.*, 'Biocathodic Methanogenic Community in an Integrated Anaerobic Digestion and Microbial Electrolysis System for Enhancement of Methane Production from Waste Sludge', *ACS Sustainable Chem. Eng.*, vol. 4, no. 9, pp. 4913–4921, Sep. 2016, doi: 10.1021/acssuschemeng.6b01221.

[39] J. C. Quintero-Díaz and J. O. Gil-Posada, 'Batch and semi-continuous treatment of cassava wastewater using microbial fuel cells and metataxonomic analysis', *Bioprocess Biosyst Eng*, vol. 47, no. 7, pp. 1057–1070, Jul. 2024, doi: 10.1007/s00449-024-03025-0.

[40] S. J. Satinover, M. Rodriguez, M. F. Campa, T. C. Hazen, and A. P. Borole, 'Performance and community structure dynamics of microbial electrolysis cells operated on multiple complex feedstocks', *Biotechnol Biofuels*, vol. 13, no. 1, p. 169, Oct. 2020, doi: 10.1186/s13068-020-01803-y.

[41] P. Batlle-Vilanova *et al.*, 'Assessment of biotic and abiotic graphite cathodes for hydrogen production in microbial electrolysis cells', *International Journal of Hydrogen Energy*, vol.

39, no. 3, pp. 1297–1305, Jan. 2014, doi: 10.1016/j.ijhydene.2013.11.017.

[42] L. Lu, D. Xing, N. Ren, and B. E. Logan, 'Syntrophic interactions drive the hydrogen production from glucose at low temperature in microbial electrolysis cells', *Bioresource Technology*, vol. 124, pp. 68–76, Nov. 2012, doi: 10.1016/j.biortech.2012.08.040.

[43] L. Cristiani *et al.*, 'Enhancing energy efficiency and H2 production in lab-scale dual chamber microbial electrolysis cells: A focus on catholyte composition and voltage losses', *Journal of Environmental Chemical Engineering*, vol. 12, no. 1, p. 111782, Feb. 2024, doi: 10.1016/j.jece.2023.111782.

[44] T. H. J. A. Sleutels, S. D. Molenaar, A. T. Heijne, and C. J. N. Buisman, 'Low Substrate Loading Limits Methanogenesis and Leads to High Coulombic Efficiency in Bioelectrochemical Systems', *Microorganisms*, vol. 4, no. 1, Jan. 2016, doi: 10.3390/microorganisms4010007.

[45] I. Ivanov, L. Ren, M. Siegert, and B. E. Logan, 'A quantitative method to evaluate microbial electrolysis cell effectiveness for energy recovery and wastewater treatment', *International Journal of Hydrogen Energy*, vol. 38, no. 30, pp. 13135–13142, Oct. 2013, doi: 10.1016/j.ijhydene.2013.07.123.

[46] L. Zhang, Y. Bai, J. Sang, J. Dong, X. Wu, and Q. Ban, 'Enhanced Biohydrogen Production through Dark Fermentation by Humic Acid: Insights into Microbial Composition and Functional Genes', *J Microbiol Biotechnol*, vol. 35, p. e2412071, Jun. 2025, doi: 10.4014/jmb.2412.12071.

[47] R. Abdallah *et al.*, 'Dark fermentative hydrogen production by anaerobic sludge growing on glucose and ammonium resulting from nitrate electroreduction', *International Journal of Hydrogen Energy*, vol. 41, no. 12, pp. 5445–5455, Apr. 2016, doi: 10.1016/j.ijhydene.2016.02.030.